Quantitative Measurements of Frictional Properties of *n*-Alkanethiols on Au(111) by Scanning Force Microscopy

Lingyan Li, Qiuming Yu, and Shaoyi Jiang*

Department of Chemical Engineering, Kansas State University, Manhattan, Kansas 66506

Received: February 23, 1999; In Final Form: July 26, 1999

We present a quantitative study of the frictional properties of self-assembled alkanethiol monolayers on Au(111) as a function of chain length using scanning force microscope. The lateral and normal forces are calibrated *in situ* using a combination of the two-slope method proposed by Ogletree *et al.* and the added mass method proposed by Cleveland *et al.* The comparative study of the same system by another calibrated Si_3N_4 tip was carried out. The friction coefficients for the same alkanethiol system, but with different tips, differ by less than 15%, indicating the reliability of nanoscale frictional and normal force measurements using a scanning force microscope. An *in situ* experimental force calibration for each cantilever is needed in order to perform absolute force measurements. Our results also show that frictional forces depend strongly on the number of carbon atoms in the alkane chain. The friction coefficient of alkanethiol decreases as the chain length increases and is lower than that of a bare Au(111) surface.

Introduction

An understanding of the microscopic phenomena that control adhesion, friction, and lubrication is extremely important.[1,2] Scanning force microscope (SFM)[3,4] is an ideal instrument to study the phenomena down to the atomic scale. The advantage of SFM is that it allows the accurate measurements of forces applied in the horizontal as well as normal directions to the surface in addition to providing atomic-scale resolution images. The SFM tip has a radius of 20−100 nm, thus, it can be considered as a model single asperity for tribological studies. Recently, SFM has been widely used to study the surfaces covered with thin organic layers.

Self-assembled monolayers (SAMs) have been of great interest in recent years due to their potential use as boundary lubricants in several technological applications, such as information storage devices and microelectromechanical systems (MEMS).[5−8] The most commonly studied system of SAMs is alkanethiol ($CH_3-(CH_2)_{n-1}-SH$) on Au(111) substrate. Previous studies of SAMs have focused on the film/substrate preparation and SAM quality characterization by various techniques.[9−12] There is not much understanding on how the quality of the grafted layer will affect tribological properties of the system. Moreover, many results emerging from SFM studies are the outcomes of incompletely characterized methodologies. Without careful calibrations, SFM results may be difficult to reproduce and interpret.

Recently, several groups have studied the frictional properties of alkanethiols on Au(111) substrate using SFM.[13−15] Lio et al.[13] reported a comparative study of the frictional properties of alkanethiols/Au(111) as a function of chain length. In their work, the normal force constant was estimated from a continuum elasticity model after measuring the cantilever critical dimensions by SEM.[16] The lateral force calibration was derived from an estimate of the relative deflection due to bending and twisting of the cantilever.[16] The lateral deflection sensitivity was assumed equal to the normal deflection sensitivity. Their results show that the frictional behavior is very similar with more than 8−11 carbons in the chain. However, C_{12} thiol yields lower frictional forces than C_{18} thiol. In the other work by McDermott et al.,[14] it was shown that the friction coefficient decreases as the chain length increases. In their work, the normal force constant was calculated using the physical and material specifications provided by cantilever manufacturers while the torsional force constant was calculated by approximating the cantilever as two parallel beams.[17] The lateral deflection sensitivity was determined from the slopes at the stationary turnaround points of the friction loop, which is valid only for hard surfaces.[18] Frictional forces from Lio et al.[13] and McDermott et al.[14] differ by as large as 1 order of magnitude for the same system under the same load. These two groups are among the first to systematically study the relationship between frictional force and chain length. Recently, Kim et al.[15] investigated the effect of chain termination on frictional properties and found that the difference in friction arises predominantly from the difference in the size of the terminal groups. The application of SFM in the study of frictional properties has been carried out on other SAMs,[13,19,20] Langmuir−Blodgett films,[8,21] polymers,[22] solid surfaces,[4] and alkanethiols/Au(111) with chemically modified tips.[23−26]

While many striking qualitative properties are revealed in friction data, a fundamental understanding of these phenomena requires a quantitative analysis. Most of previous studies use formulas or calculations based on numerical methods to estimate the normal and lateral force constants.[16,27−30] These calculations require the dimensions and relevant elastic moduli of the cantilever, which are not easy to measure. Measurements of nanoscale friction and adhesion based on calculated force constants are unlikely to yield reproducible results with different tips. Thus, comparative studies are often carried out using the same tip. Recently, Ogletree et al.[16] have presented the only in situ method for lateral force calibration, assuming that the normal force is known. Some nondestructive in situ methods for normal force constant calibration have been successfully

* To whom correspondence should be addressed. E-mail: sjiang@pluto.cheme.ksu.edu.

10.1021/jp990645p CCC: $18.00
Published on Web 09/09/1999

implemented. Examples include measuring the deflections or resonance frequency shifts for a cantilever loaded with known masses[31] and measuring the deflection of the cantilever when in contact with another cantilever of known force constant.[32] Of these methods, the added mass method proposed by Cleveland et al.[31] has been widely used for normal force calibration.

The objectives of this study are to combine the two-slope and the added-mass methods for quantitative frictional and normal force measurements and to demonstrate the reliability of nanoscale frictional and normal force measurements. Although the frictional properties of the alkanethiol/Au(111) system have been studied as a function of chain length by several groups before,[13,14] to the best of our knowledge, it is the first time that absolute force measurements based on the in situ force calibration methods have been achieved.

Experiments

Materials. Alkanethiols were purchased from Aldrich Chemical Co., Inc. (Milwaukee, WI) (C_8, C_{12}, and C_{18}) and used as received. Glassware for the preparation of SAMs was cleaned with chromic acid cleaning solution (Fisher Scientific). House-distilled water was passed through a purification unit producing a resistivity of 18.0 MΩ cm. A 1.0 mm polycrystalline gold wire (99.9985%) was purchased from Alfa Æsar. Glass beads from Polyscience were used for the normal force calibration. The faceted $SrTiO_3$ (305) surface was used for the lateral force calibration. The $SrTiO_3$ crystal from the Universite de Lausanne (Switzerland) was annealed for 20 h at 1100 °C in flowing oxygen as discussed in the literature.[34]

Monolayer Preparation. Gold substrates were prepared by annealing a gold wire in a H_2/O_2 flame.[33] The gold wire was first cleaned by dipping into piranha solution (3:1 concentrated H_2SO_4/30% H_2O_2) several times and rinsing with pure water. The wire was then placed in a H_2/O_2 flame and allowed to melt until an approximately 1.5−2.0 mm diameter droplet had formed at the end of the wire. The droplet was further annealed for a short time in a cooler part of the flame. The resulting gold facet shows large flat terraces and monatomic steps under SFM. Immediately after removal from the flame the gold droplet was immersed in a 1 mM ethanol solution of alkanethiol. The gold substrate was left in the solution at room temperature for at least 36 h and then rinsed with ethanol and dried in a N_2 stream.

SFM Measurements. Experiments were carried out with a multimode SFM (Digital Instrument, Santa Barbara, CA). Commercially available 100 μm long, 36 μm wide, gold-coated, V-shaped Si_3N_4 cantilevers with a nominal force constant of 0.58 N/m (DI) were used. The microscope was operated in constant force mode. To minimize the thermal drift, the instrument was allowed to equilibrate for 3−4 h before any data collection. The piezo scanner sensitivity for the $x-y$ directions was calibrated from lattice resolution images of mica and Au(111). The Z piezo calibration was determined by the two-slope method[16] and from a monatomic step height on Au(111) substrate.

Large-scale topographical image of SAM (1 μm × 1 μm) was captured to determine the monatomic terrace. Atomic resolution images were obtained and frictional forces under a certain applied load were measured on the terrace. The 10 nm trace−retrace cycle of a friction loop shows the sawtooth behavior. The scan rate is 360∼600 nm/s for all smaller scale (≤10 nm × 10 nm) experiments. The normal force signals between tip and sample, $F_{N,0}$, were determined from the ASCII files of the normal force signal versus z-displacement curves. The frictional signals, $F_{L,0}$, were collected from the ASCII files of the friction loops.

Force Calibrations. Quantitative and reproducible measurements of nanoscale forces with SFM require an accurate (preferably in situ) calibration of both lateral and normal forces. To convert experimental normal ($F_{N,0}$) and lateral ($F_{L,0}$) deflection signals in voltage into normal (F_N) and lateral (F_L) forces in Newtons, one has to obtain normal force calibration factor β and lateral force calibration factor α, having the unit of nN/V.

$$F_N = k_N \Delta z = k_N c_N F_{N,0} = \beta F_{N,0}$$
$$F_L = k_L \Delta x = k_L c_L F_{L,0} = \alpha F_{L,0} \quad (1)$$

where k_N and k_L are normal and lateral force constants, Δz and Δx are normal and lateral displacements of the cantilever, and c_N and c_L are normal and lateral force optical deflection sensitivities. We combined the two-slope and added-mass methods to obtain the lateral and normal force calibration factors α and β. The ratio α/β was determined by the two-slope method developed by Ogletree et al.[16] The k_N was determined by the added mass method proposed by Cleveland et al.,[31] while the c_N was determined by measuring the slope of the normal force signal versus z-displacement curve on a hard surface. The product of k_N and c_N gives β. Thus, the value of the lateral force calibration factor α can be obtained once α/β and β are known.

The two-slope method using a $SrTiO_3$(305) surface was carried out to obtain the α/β ratio. The faceted $SrTiO_3$(305) surface has (101) and (103) planes that tilt +14.0° and −12.5° with respect to the original (305) surface.[16,34] As the top of $SrTiO_3$ ridges is extremely sharp,[34] a topographic scan over a ridge produces an image of the tip. Thus, the $SrTiO_3$ sample can be also used to evaluate the tip quality.[34] The ridges are typically 5−20 nm high and are spaced 10−100 nm apart. We carefully chose the widest facets to measure lateral signals as a function of load for the cantilever lateral force calibration. The calculation of α/β from the lateral signals will be discussed in the next section and in the Appendix. The equations and calculation procedures are given in the Appendix.

The added mass method is used for the cantilever normal force calibration. When a mass M is added at the end of the cantilever, the resonant frequency (ν) is given by[35]

$$\nu = \frac{\omega}{2\pi} = \frac{1}{2\pi}\sqrt{\frac{k_N}{M + m^*}} \quad (2)$$

where m^* is the effective mass of the beam and k_N is the normal force constant of the cantilever. The equation is rearranged to give

$$M = k_N(2\pi\nu)^{-2} - m^* \quad (3)$$

Equation 3 shows that if several known masses are added to the end of the cantilever and the new resonant frequencies are measured, a plot of added mass versus $(2\pi\nu)^{-2}$ gives a straight line with the slope being the force constant. In this study, glass beads were used as added masses to cantilevers. The mass of a particle was calculated based on the sphere radius measured by SEM and the bulk density of glass, 2.5 g/cm^3. The tip was used as a micromanipulator to pick up a glass bead. The adhesion between a glass bead and a Si_3N_4 tip is strong enough to move and then secure the sphere to the cantilever. Several measurements were made using glass beads of diameters from 15.2 to 36.2 μm on a cantilever.

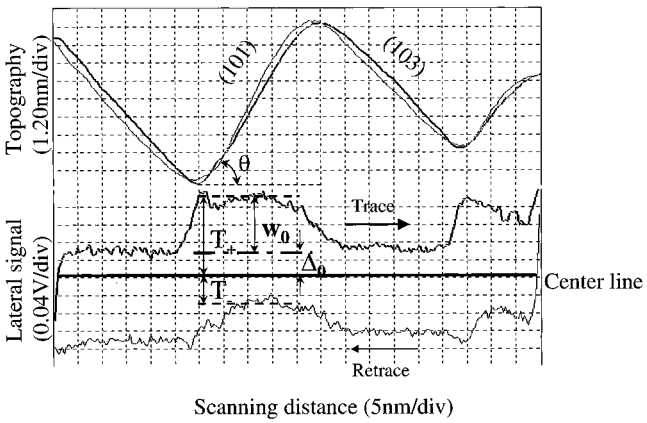

Figure 1. Experimental lateral signals (T_0) measured on the (101) and (103) facets of the $SrTiO_3$ (305) surface versus scan distance for trace and retrace directions at a given load. W_0 and Δ_0 are calculated from the friction loop. The simultaneously acquired topography (upper image) is also shown.

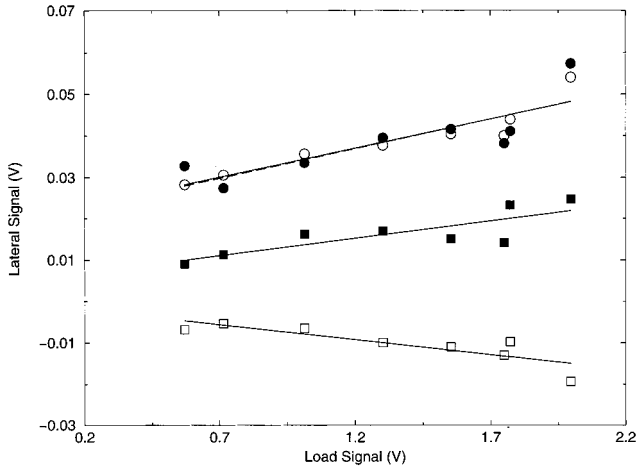

Figure 2. Friction loop half-widths $W_0(101)$ (●) and $W_0(103)$ (○) and offsets $\Delta_0(101)$ (■) and $\Delta_0(103)$ (□) as a function of load signal for the (101) and (103) facets. The slopes of each line are calculated and used to calculate the ratio of α/β. The resulting ratio of α/β for this cantilever (tip 1) is 38.5.

The normal force optical deflection sensitivity, c_N, was determined from the slope of the linear part of the normal force signal versus *z*-displacement curve. It is necessary to obtain a new c_N each time when a new probe is mounted or the optical beam is realigned.

Results and Discussion

Figure 1 shows an example of the simultaneously acquired topography and lateral deflection signals from a single line scan on the (101) and (103) facets of the $SrTiO_3$(305) surface. Friction loop half-widths $W_0(101)$ and $W_0(103)$ and offsets $\Delta_0(101)$ and $\Delta_0(103)$ were calculated from the friction loop. A series of measurements of W_0 and Δ_0 over a range of total loads are shown in Figure 2. The slopes of the curves, $W_0'(101)$, $W_0'(103)$, $\Delta_0'(101)$, and $\Delta_0'(103)$, were used to calculate the ratio of α/β using the equations and procedure given in the Appendix. We determined the ratio of α/β for two tips fabricated from the same wafer. The resulting values of α/β are given in Table 1. Figure 3 shows an example of the added mass versus $(2\pi\nu)^{-2}$ for tip 1. The normal force constants for two tips are determined from the slopes of the curves and are also given in Table 1. To yield reproducible results, such an experimental force calibration for each cantilever is important.

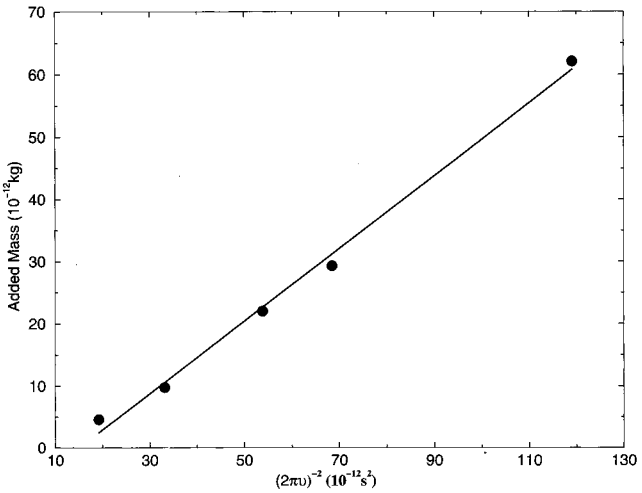

Figure 3. A plot of added mass vs $(2\pi\nu)^{-2}$ for tip 1. The linear regression of the data gives a force constant of 0.584 N/m with a correlation coefficient of 0.9973.

TABLE 1: Experimental Cantilever Calibration Results

	α/β	k_N (N/m)
tip 1	39 ± 4	0.58 ± 0.03
tip 2	36 ± 3	0.53 ± 0.08

The quality of the prepared SAMs was first examined. Figure 4 is a large-scale (500 nm × 500 nm) topographic image of the SAM. The films were featureless on this scale except the appearance of terraces resulting from the steps in the underlying gold substrate, indicating well-formed monolayer structures. A monatomic step was measured to be 0.24 nm in height from the section analysis, as shown in Figure 4. Thiolate monolayers on Au(111) with chain lengths above 8−12 carbons self-assemble to form very sturdy layers. On an atomic flat terrace, a small scale scan (6 nm × 6 nm) revealed molecular-level features in the frictional force image. Figure 5 shows a frictional image of octadecanethiol SAM and its corresponding fast Fourier transform (FFT) spectra, showing a $(\sqrt{3} \times \sqrt{3})$R30° hexagonal order structure with respect to the 1 × 1 structure of Au(111) with 0.499 nm periodicity. The SFM lattice-resolved image of the octadecanethiol monolayer agrees with that of other techniques.[36] Our experiments also show that the layer will become disordered and eventually be displaced by the SFM tip under high external loads as observed previously.[37]

With tips calibrated *in situ* by the combined two-slope and added-mass methods, we measured the frictional properties of alkanethiols on Au(111) and of a bare Au(111) surface as a function of total load at the nanometer scale, demonstrating the reliability of nanoscale force measurements with the calibrated tips. Figure 6 shows frictional force versus total load curves for two calibrated Si_3N_4 tips scanning over different SAMs. The zero point of total load is defined as the point where the tip breaks contact with the surface. That is, F_N is the sum of adhesion force (capillary forces, molecular interactions) and external applied load. The frictional forces were investigated for the total loads up to 60 nN in an effort to probe the frictional properties of only the outermost portions of the SAMs. The higher loads will cause damage on the monolayers. Hysteresis in the measured friction is small. Thus, the data points obtained upon decreasing loads are not shown. As seen in Figure 6, an approximately linear response is observed for the range of loads investigated. The friction curves for C_{18}, C_{12}, and C_8 layers lie well below that for a bare Au(111) surface. Furthermore, friction increases as the chain length decreases due to the increased

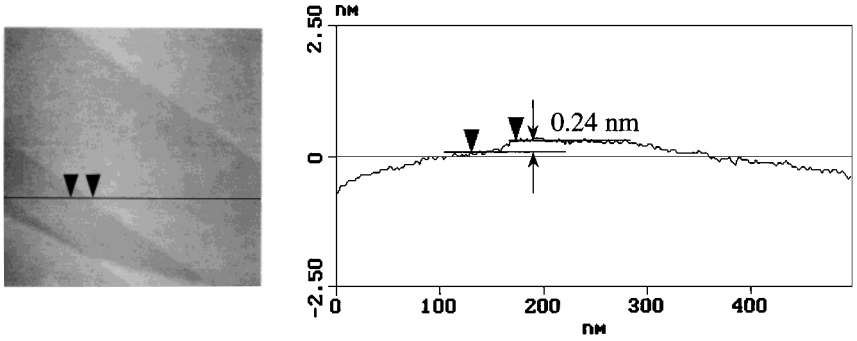

Figure 4. SFM topographic image of self-assembled octadecanethiol monolayer on Au(111) surface. The section analysis shows that the steps are monatomic, i.e., 0.24 nm in height.

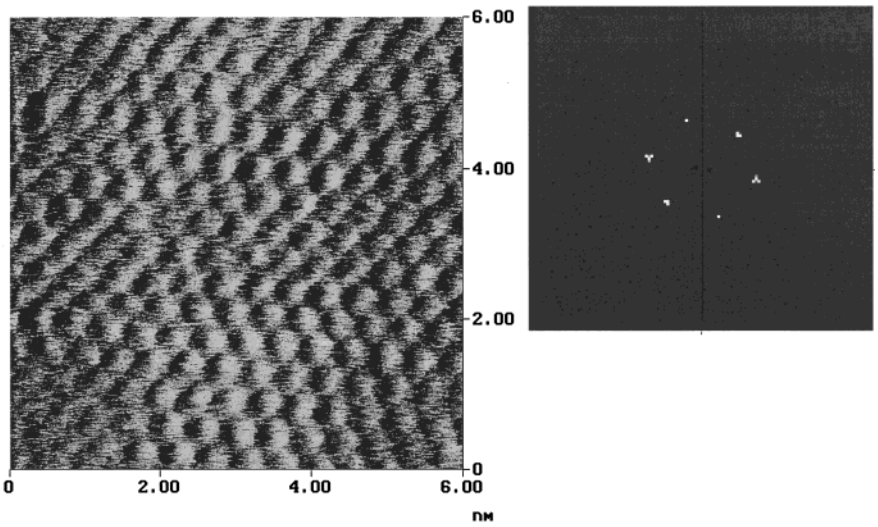

Figure 5. Frictional force image for octadecanethiol on Au(111) and the corresponding FFT spectra. Scanning speed is 360 nm/s.

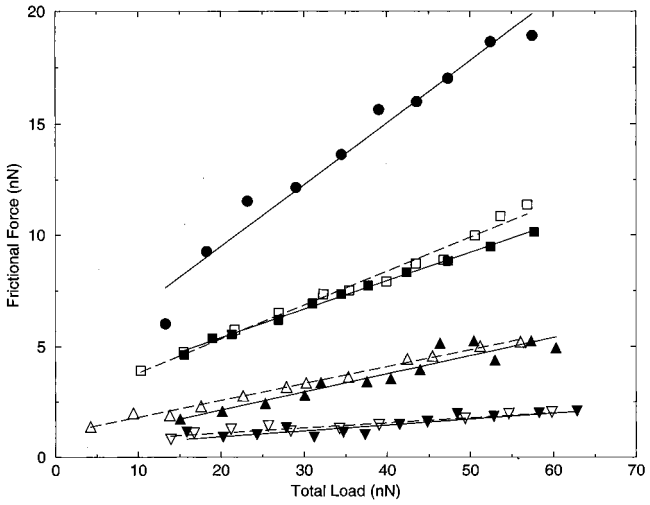

Figure 6. Frictional force vs load curves for two calibrated Si_3N_4 tips scanning over C_{18}, C_{12}, and C_8 alkanethiol monolayers on Au(111). A curve for bare Au(111) is also shown as a reference. Solid lines and filled symbols represent the linear regression and the raw data points obtained using tip 1. Dashed lines and open symbols represent the linear regression and the raw data points obtained using tip 2: (●) Au(111); (■) C_8-thiol; (▲) C_{12}-thiol; (▼) C_{18}-thiol.

disorder of the films.[13,15] We also carried out molecular dynamics simulation studies of frictional properties of C_{12} and C_{18} thiols on Au(111) scanned by a Si_3N_4 tip as a function of applied load. Our preliminary results[38] show that C_{12} thiol produces higher friction than its C_{18} counterpart as found in

TABLE 2: Friction Coefficients, μ, Obtained from the Linear Regression of Frictional Force versus Load Curves Shown in Figure 6

	Au(111)	C_8-thiol	C_{12}-thiol	C_{18}-thiol
tip 1[a]	0.28 ± 0.03	0.13 ± 0.01	0.081 ± 0.009	0.027 ± 0.003
tip 2[a]		0.15 ± 0.01	0.076 ± 0.006	0.023 ± 0.002

[a] α/β and k_N of tip 1 and tip 2 are given in Table 1.

experiments. To demonstrate the reliability of the *in situ* calibration methods, the friction versus load curves were also measured by using the second calibrated tip. The results are shown in Figure 6. As we can see, the friction curves obtained from both tips agree quite well. The friction coefficients from our experiments are presented in Table 2. The friction coefficients differ by less than 15% for the same system with different tips. The results show that, with *in situ* force calibration, different tips yield comparable frictional forces. Measurements using tips either without calibration or with estimated force constants are unlikely to yield reproducible results. Quantitative measurements of frictional forces using SFM rely on many factors such as reliable calibration methods, the nature (e.g., functionality and geometry) of tips, and the environment. With the two tips used in this work from the same wafer, the similarity between the two tips could be expected. Thus, they should generate the similar frictional properties. The reproducibility of the frictional properties is not expected if the nature of tips is different.

We notice the nonlinear part of friction vs total load curves in the low load regime (below ~10 nN). The linear variation

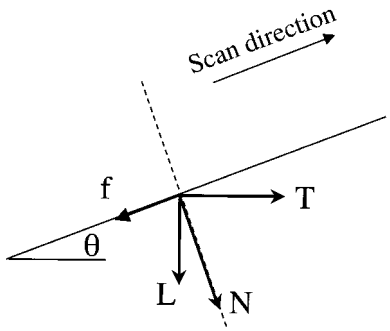

Figure 7. Forces exerted on the surface by the SFM tip while scanning up a sloped surface.

of nanoscale friction force with total load is valid only for loads in the range of about 10−60 nN for our system. The Hertzian contact model in the elastic regime predicts a $L^{2/3}$ law for a spherical tip and a $L^{1/2}$ law for a conical tip. This was observed in the earlier work on mica by Hu et al.[39] The nonlinearity of the frictional force versus load at very low loads might correspond to the dominance of elastic deformations.

All our experiments were carried out in air with humidity around 30%. A homemade chamber for humidity and temperature control was built recently in our laboratory for the further exploration of the frictional properties of pure and mixed SAMs.

Conclusions

We present a quantitative study of the frictional behavior of self-assembled alkanethiol monolayers on Au(111) substrate using scanning force microscope in the wearless regime. Lateral and normal forces are calibrated *in situ* by combined two-slope and added-mass methods, leading to quantitative and reliable measurements of nanoscale forces. Our results also show that the friction curves for C_{18}, C_{12}, and C_8 layers lie well below that for a bare Au(111) surface and the friction coefficient increases as the chain length decreases as found previously by other workers.

Appendix

Two-Slope Method. The two-slope method was developed by Ogletree et al.[16] for the lateral force calibration. The friction−load relation for a Si_3N_4 tip on a $SrTiO_3$(305) surface was found to be well represented by a linear form,

$$f = \mu N \tag{A1}$$

where f is the force parallel to the surface, μ is the friction coefficient, and N is the force normal to the surface. As the tip scans up or down a sloped surface, the vertical load L and the horizontal force T were balanced by f and N, as shown in Figure 7 and described by the following equations:

$$\begin{aligned} N_{\pm} &= L\cos\theta \pm T_{\pm}\sin\theta \\ f_{\pm} &= T_{\pm}\cos\theta \mp L\sin\theta \end{aligned} \tag{A2}$$

where + denotes uphill motion and − downhill motion. θ is the tilt angle of the (101) or (103) plane with respect to the original (305) surface. Experimentally, we measure T_0 and L_0, where $T = \alpha T_0$ and $L = \beta L_0$ (the "0" subscript indicates a force measured in transducer output volts rather than newtons). The half-width W and the offset Δ of the friction loop are calculated from $W = (T_+ + T_-)/2$ and $\Delta = (T_+ - T_-)/2$, respectively. Experimentally, one measures lateral forces for a range of applied loads, plots W and Δ against L, and obtains the slopes $\Delta' = d\Delta/dL$ and $W' = dW/dL$. From eqs A1 and A2, these slopes are given by

$$\frac{\alpha}{\beta}\Delta_0' = \Delta' = \frac{(1+\mu^2)\sin\theta\cos\theta}{\cos^2\theta - \mu^2\sin^2\theta} \tag{A3a}$$

and

$$\frac{\alpha}{\beta}W_0' = W' = \frac{\mu}{\cos^2\theta - \mu^2\sin^2\theta} \tag{A3b}$$

The ratio of eqs A3a and A3b gives

$$\mu + \frac{1}{\mu} = \frac{2\Delta_0'}{W_0'\sin 2\theta} \tag{A3c}$$

The ratio of α/β can be obtained if eqs A3b and A3c are applied to (101) and (103) planes and experimentally measured quantities $W_0'(101)$, $W_0'(103)$, $\Delta_0'(101)$, and $\Delta_0'(103)$ are known. The calculation procedure is as follows.

(1) Guess an initial μ_{103}.

(2) Calculate μ_{101} from eq A4,

$$\mu_{101} = \frac{-1 + \sqrt{1 + \kappa^2\sin^2\theta_{101}}}{2\kappa\sin^2\theta_{101}} \tag{A4}$$

where

$$\kappa \equiv p\frac{\mu_{103}}{\cos^2\theta_{103} - {\mu_{103}}^2\sin^2\theta_{103}}$$

$$p \equiv \frac{W_0'(101)}{W_0'(103)} = \frac{W_{101}'}{W_{103}'}$$

(3) Go to step 4 if eq A5 is satisfied. Otherwise, modify μ_{103} and return to step 2.

$$2q = \left(\frac{1}{\mu_{101}} + \mu_{101}\right)\sin 2\theta_{101} - \left(\frac{1}{\mu_{103}} + \mu_{103}\right)\sin 2\theta_{103}\frac{1}{p} \tag{A5}$$

where

$$q \equiv \frac{\Delta_0'(101) - \Delta_0'(103)}{W_0'(101)} = \frac{\Delta_{101}' - \Delta_{103}'}{W_{101}'}$$

(4) Determine the ratio of α/β from eq A6.

$$\frac{\alpha}{\beta} = \frac{1}{W_0'(103)}\frac{\mu_{103}}{\cos^2\theta_{103} - {\mu_{103}}^2\sin^2\theta_{103}} \tag{A6}$$

Acknowledgment. We thank M. Salmeron for his encouragement and help. We also thank J. P. Cleveland, S. S. Perry, M. T. McDermott, S. Clear, and H. T. Kim for helpful discussions. This work is supported by the National Science Foundation (CTS-9815436), the NSF/EPSCoR program, and the Advanced Manufacturing Institute of the State of Kansas.

References and Notes

(1) Carpick, R. W.; Salmeron, M. *Chem. Rev.* **1997**, *97*, 1163.

(2) Bhushan, B.; Israelachvili, J. N.; Landman, U. *Nature* **1995**, *374*, 607.

(3) Binnig, G.; Quate, C. F.; Gerber, C. *Phys. Rev. Lett.* **1986**, *56*, 930.

(4) Mate, C. M.; McClelland, G. M.; Erlandsson, R.; Chiang, S. *Phys. Rev. Lett.* **1987**, *59*, 1942.

(5) Howe, R. T. *J. Vac. Sci. Technol.* **1988**, *B6*, 1809.
(6) Miu, D. K.; Wu, S.; Temesvary, V.; Tai, Y.-C. *Adv. Info. Storage Syst.* **1993**, *5*, 139.
(7) Zarrad, H.; Clechett, P.; Belin, M.; Martelet, C.; Jaffrezic-Renault, N. *J. Micromech. Microeng.* **1993**, *3*, 222.
(8) Bhushan, B.; Kulkarni, A. V.; Koinkar, V. N.; Boehm, M.; Odoni, L.; Martelet, C.; Belin, M. *Langmuir* **1995**, *11*, 3189.
(9) Nuzzo, R. G.; Allara, D. L. *J. Am. Chem. Soc.* **1983**, *105*, 4481.
(10) Whitesides, G. M.; Ferguson, G. S. *Chemtracts* **1988**, *1*, 171.
(11) Chidsey, C. E. D.; Liu, G.; Rowntree, P.; Scoles, G. *J. Chem. Phys.* **1989**, *91*, 4421.
(12) Nuzzo, R. G.; Dubois, L. H.; Allara, D. L. *J. Am. Chem. Soc.* **1990**, *112*, 558.
(13) Lio, A.; Charych, D. H.; Salmeron, M. *J. Phys. Chem. B* **1997**, *101*, 3800.
(14) McDermott, M. T.; Green, J.-B. D.; Porter, M. D. *Langmuir* **1997**, *13*, 2504.
(15) Kim, H. I.; Koini, T.; Lee, T. R.; Perry, S. S. *Langmuir* **1997**, *13*, 7192.
(16) Ogletree, D. F.; Carpick, R. W.; Salmeron, M. *Rev. Sci. Instrum.* **1996**, *67*, 3298.
(17) O'Shea, S. J.; Welland, M. E.; Wong, T. M. H. *Ultramicroscopy* **1993**, *52*, 55.
(18) Carpick, R. W.; Ogletree, D. F.; Salmeron, M. *Appl. Phys. Lett.* **1997**, *70*, 1548.
(19) Liu, Y.; Wu, T.; Evans, D. F. *Langmuir* **1994**, *10*, 2241.
(20) Xiao, X.; Hu, J.; Charych, D. H.; Salmeron, M. *Langmuir* **1996**, *12*, 235.
(21) Meyer, E.; Overney, R.; Brodbeck, D.; Howald, L.; Luthi, R.; Frommer, J.; Guntherodt, H.-J. *Phys. Rev. Lett.* **1992**, *69*, 1777. Overney, R. M.; Meyer, E.; Frommer, J.; Guntherodt, H.-J.; Decher, G.; Sohling, U. *Langmuir* **1993**, *9*, 341.
(22) O'Shea, S. J.; Welland, M. E.; Rayment, T. *Langmuir* **1993**, *9*, 1826.
(23) Frisbie, C. D.; Tozsnyai, L. F.; Noy, A.; Wrighton, M. S.; Lieber, C. M. *Science* **1994**, *265*, 2071.
(24) Noy, A.; Frisbie, C. D.; Rozsnyai, L. F.; Wrighton, M. S.; Lieber, C. M. *J. Am. Chem. Soc.* **1995**, *117*, 7943.
(25) Noy, A.; Vezenov, D. V.; Lieber, C. M. *Annu. Rev. Mater. Sci.* **1997**, *27*, 381.
(26) Green, J. B. D.; McDermott, M. T.; Porter, M. D.; Siperko, L. M. *J. Phys. Chem.* **1995**, *99*, 10960.
(27) Albrecht, T. R.; Akamine, S.; Carver, T. E.; Quate, C. F. *J. Vac. Sci. Technol. A* **1990**, *8*, 3386.
(28) Butt, H.-J.; Siedle, P.; Seifert, K.; Fendler, K.; Deeger, T.; Bamberg, E.; Weisenhorn, A. L.; Goldie, K.; Engel, A. *J. Microsc.* **1993**, *169*, 75.
(29) Neumeister, J. M.; Ducker, W. A. *Rev. Sci. Instrum.* **1994**, *65*, 2527.
(30) Sader, J. E. *Rev. Sci. Instrum.* **1995**, *66*, 4583.
(31) Cleveland, J. P.; Manne, S. Bocek, D. Hansma, P. K. *Rev. Sci. Instrum.* **1993**, *64*, 403. Sader J. E.; Larson, I.; Mulvaney, P.; White, L. R. *Rev. Sci. Instrum.* **1995**, *66*, 3789.
(32) Ruan, J. A.; Bhusan, B. *Trans. ASME J. Tribol.* **1994**, *116*, 378. Li, Y. Q.; Tan, N. J.; Pan, J.; Garcia, A. A.; Lindsay, S. M. *Langmuir* **1993**, *9*, 637. Gibson, C. T.; Watson, G. S.; Myhra, S. *Nanotechnology* **1996**, *7*, 259.
(33) Clavilier, J.; Armand, D.; Wu, B. L. *J. Electroanal. Chem. Interfacial Electrochem.* **1982**, *135*, 159. Hidetoshi, H.; Sugawara, S.; Itaya, K. *Anal. Chem.* **1990**, *62*, 2424. Hayes, W. A.; Shannon, C. *Langmuir* **1998**, *14*, 1099.
(34) Sheiko, S. S.; Möller, M.; Reuvekamp, E. M. C. M.; Zandbergen, H. W. *Phys. Rev. B* **1993**, *48*, 5675.
(35) Stokey, W. F. *Shock and Vibration Handbook*; McGraw-Hill: New York, 1989.
(36) Strong, L.; Whitesides, G. M. *Langmuir* **1988**, *4*, 546.
(37) Liu, G.; Salmeron, M. B. *Langmuir* **1994**, *10*, 367.
(38) Balasundaram, R.; Li, L.; Jiang, S. Annual AIChE Meeting, Miami, FL, November, 1998.
(39) Hu, J.; Xiao, X.; Ogletree, D. F.; Salmeron, M. *Surf. Sci.* **1995**, *327*, 358.